Published in final edited form as:

ACS Appl Mater Interfaces. 2017 January 25; 9(3): 2196–2204. doi:10.1021/acsami.6b15291.

Prevascularization of Decellularized Porcine Myocardial Slice for Cardiac Tissue Engineering

Pawan KC[†], **Mickey Shah**[†,‡], **Jun Liao**[§], and **Ge Zhang**[*,†]

† Department of Biomedical Engineering, The University of Akron,Akron, Ohio 44325, United States

‡ Integrated Bioscience Program, The University of Akron, Akron, Ohio 44325, United States

§ Department of Bioengineering, University of Texas at Arlington, Arlington, Texas 76019, United States

Abstract

Prevacularization strategies have been implemented in tissue engineering to generate microvasculature networks within a scaffold prior to implantation. Prevascularizing scaffolds will shorten the time of functional vascular perfusion with host upon implantation. In this study, we explored key variables affecting the interaction between decellularized porcine myocardium slices (dPMSs) and reseeded stem cells toward the fabrication of prevascularized cardiac tissue. Our results demonstrated that dPMS supports attachment of human mesenchymal stem cells (hMSCs) and rat adipose derived stem cells (rASCs) with high viability. We found that cell seeding efficiency and proliferation are dPMS thickness dependent. Compared to lateral cell seeding, bilateral cell seeding strategy significantly enhanced seeding efficiency, infiltration, and growth in 600 μm dPMS. dPMS induced endothelial differentiation and maturation of hMSCs and rASCs after 1 and 5 days culture, respectively. These results indicate the potential of dPMS as a powerful platform to develop prevascularized scaffolds and fabricate functional cardiac patches.

Graphical Abstract

[*]**Corresponding Author** Phone: (330) 972-5237. gezhang@uakron.edu.

Notes

The authors declare no competing financial interest.

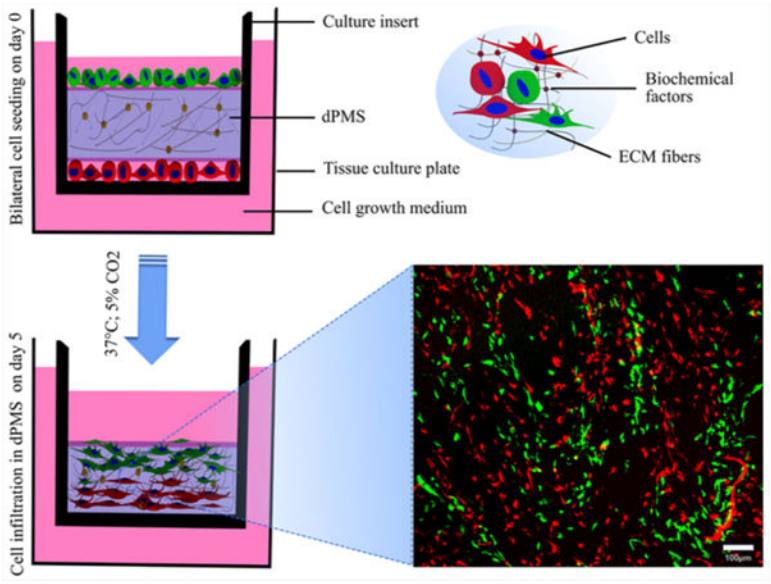

Keywords

prevascularization; decellularized extracellular matrix; cardiac tissue engineering; human mesenchymal stem cells; rat adipose derived stem cells; stem cell differentiation

1. INTRODUCTION

Prevascularization has become a promising strategy in tissue engineering to improve the survival rate of thick tissue constructs after implantation.[1–3] It aims to generate micro-vasculature networks inside the scaffold that could rapidly inosculate and anastomose with host microvasculature following implantation. Compared with in vivo vascularization, which focuses on simulating vascular ingrowth from the host, prevascularization could greatly shorten the hypoxia period after implantation and therefore avoid significant cell death. Many groups have explored various strategies that aim to enhance in vitro prevascularization of tissue engineering constructs and have shown encouraging in vivo results after implantation. For example, prevascularized fibrin construct, when implanted subcutaneously into immune-deficient Rag-2 mice, has shown to accelerate the formation of functional anastomoses with the host vasculature, leading to earlier perfusion and metabolic activity in the implanted tissue.[4] Prevascularized neonatal rat cardiac cell patch, when transplanted into the infarcted rat cardiac region, has demonstrated to be electrically coupled with host myocardium and improved the electromechanical function of the treated heart.[5] Similarly, prevascularized tissue-engineered bone construct, when tested on sheep bone defect, has been found to improve vascularization and osteogenesis.[6] These results suggest that prevascularization strategies could be used to significantly shorten the time of vascular perfusion from the host, improving the construct survival and in vivo function after implantation.

Prevascularization has been achieved through various strategies including scaffold functionalization and microelectromechanical systems (MEMS)-related approaches.[7,8]

Scaffolds have been functionalized using various pro-angiogenic factors such as vascular endothelial growth factor (VEGF), basic fibroblast growth factor (bFGF), and platelet-derived growth factor (PDGF) to promote vasculogenesis.[9–11] Although success has been made in terms of effectively loading pro-angiogenic factors to the scaffold and promoting regional vascularization via controlled release of single or multiple factors,[8] it remains a challenge to implement the knowledge of the complicated temporal and spatial expression profiles of the pro-angiogenic factors during vessel development into scaffold engineering and design. Using MEMS and microfluidic technologies to recapitulate the branching networks of the microvasculature is another popular approach being pursued in many laboratories to develop prevascularization.[7] However, these techniques generally require using nondegradable synthetic materials such as silicone or polydimethylsiloxane (PDMS), which may not be compatible with maintaining cell viability throughout the construct and matching native tissue features of mechanical strength and porosity.

Recently, decellularized extracellular matrix (ECM) derived from various tissues (e.g., cartilage, skin, lung, heart, and liver) have been widely used as a nature biomaterial template for many tissue engineering applications. Compared with other natural or synthetic scaffolds, decellularized ECM offers many unique advantages such as preserving organ specific micro-structure, mechanical properties, and biochemical cues in favor of cell attachment, growth, and tissue specific differentiation.[12–14] Decellularized cardiac ECM has also been explored to be used to facilitate cardiac repair. Human heart derived decellularized ECM has enabled the seeding and survival of human cardiomyocytes and maintained representative phenotypes of the seeded cardiomyocytes including expression of cardiomyocyte-specific markers and remained electrically synchronous within the scaffold in vitro.[15] Cardiac patches made of rat decellularized cardiac tissue and induced pluripotent stem cells (iPSCs) derived cardiac cells have been proven to improve heart function in vivo.[16] However, perfusion limitations still exist for cardiac scaffolds derived from decellularized matrix affecting the efficacy and efficiency of their applications.

Increasing evidence has suggested decellularized ECM as a suitable natural scaffold for implementing a prevascularization strategy. Several studies have reported that after proper decellularization, the vasculature tree could be preserved in decellularized ECM. By coronary perfusion with ionic detergent, Ott et al. reported the successful decellularization of a rat heart into an acellular ECM with intact geometry and perfusable vascular architecture.[17] Wang et al. also reported the preservation of vasculature structure in porcine cardiac tissue after decellularization using a frame-pin supporting system in a rotating bioreactor containing sodium dodecyl sulfate (SDS) with trypsin.[18] In addition, decellularized ECM has been proved to retain many matrix-bound growth factors including pro-angiogenic factors.[19] Without external chemical inducers, our previous study has found that human mesenchymal stem cells (hMSCs) could spontaneously differentiate into vascular lineage when cultured in cardiac hydrogels derived from decellularized porcine cardiac tissue.[20]

The aim of this study is to investigate an innovative protocol for prevascularization of decellularized cardiac tissue. Our long-term goal is to use our developed prevascularized decellularized cardiac tissue as a cardiac patch to deliver stem cells for myocardial infarction treatment. In this study, decellularized cardiac tissue from porcine heart was sliced into

different thicknesses. The influence of stem cell types, scaffold thickness, and seeding method on cell seeding, growth, and cardiovascular differentiation were investigated.

2. MATERIALS AND METHODS

2.1. Materials.

Human mesenchymal stem cells and MSCGM bullet kit were purchased from Lonza (Walkersville, MD, USA). MesenPRO RS medium kit, Glutamax, and antibiotic −antimycotic were obtained from Gibco (Carlsbad, CA, USA). Sodium dodecyl sulfate, Triton-X 100, Collagenase type II, and penicillin−streptomycin were purchased from Sigma-Aldrich (St. Louis, MO, USA). Paraffin wax (type 9), HistoPrep SH75–125D tissue embedding media, absolute ethanol (200 proof), anhydrous ethanol (histological grade), and xylenes were purchased from Fisher Scientific (Florence, KY, USA). Paraformaldehyde (4% w/v aqueous solution) was purchased from Affymetrix (Cleveland, OH, USA). Live/dead viability/cytotoxicity kit, Hoechst 33342, CellTracker CM-Dil, and CellTracker green CMFDA (5-chloromethylfluorescein diacetate) were obtained from Molecular Probes (Eugene, OR, USA). VECTASHIELD mounting medium with DAPI was purchased from Vector Laboratories Inc. (Burlingame, CA, USA). VE cadherin (H-72) antibody and von Willebrand factor (H-300) antibody were purchased from Santa Cruz Biotechnology (Dallas, TX, USA). All other primary and secondary antibodies were purchased from Abcam (Cambridge, MA, USA). All materials were used as received from the manufacturer.

2.2. Preparation of Decellularized Porcine Myocardium Slices.

Fresh porcine hearts were obtained from a local slaughter house. Decellularization of porcine myocardium tissue was performed following a previously established protocol.[17,20] Briefly, native myocardium tissue was cut into ~2 cm (length) × 2 cm (width) × 1 cm (thickness) blocks and rinsed extensively in deionized (DI) water to remove excess blood. The tissue blocks were then decellularized using detergent containing 1% (w/v) sodium dodecyl sulfate (SDS) and 0.5% penicillin−streptomycin for 2.5 weeks. Subsequently, the decellularizing tissue blocks were washed with 0.01% Triton-X 100 in 1× PBS solution for 1 h, followed by thorough washing with 1× PBS for 2 days. Immediately after decellularization, the myocardium tissues were either used for experiments or stored at −20 °C until use. Cryosectioning of native and decellularized porcine myocardium tissues were performed to obtain 300, 600, and 900 μm thick slices. Prior to cryosection, the samples were embedded using HistoPrep SH75–125D tissue embedding media. After sectioning, the decellularized porcine myocardium slices (dPMSs) were sterilized using molecular biology grade absolute ethanol (200 proof) followed by at least three washes with sterilized DI water.

2.3. Cell Culture.

Human mesenchymal stem cells (hMSCs) were cultured in MSCGM bulletkit supplemented with 1% antibiotic− antimycotic. Rat adipose derived stem cells (rASCs) were isolated from subcutaneous white adipose tissues as previously described.[21,22] All animal procedures were conducted in accordance with the guidelines set by the Animal Care and Use Committee (IACUC) at the University of Akron and in compliance with standards issued by the United

States Department of Agriculture, Public Health Service, and the American Association for Accreditation of Laboratory Animal Care. In brief, subcutaneous white adipose tissues from abdomen of rat were harvested, minced, and digested enzymatically with collagenase type II (0.1% w/v) at 37 °C for 1 h, followed by centrifugation at 250*g* for 5 min to obtain the pellet containing stromal vascular fraction (SVF). The SVF was then cultured in MesenPRO RS medium kit supplemented with glutamax and 1% antibiotic−antimycotic to isolate rASCs. Both cells were maintained in a humidified cell culture incubator at 37 °C and 5% CO_2 with media change every 2 days. All experiments were performed using hMSCs at passages 5−8 and rASCs at passages 2−5.

2.4. Cell Reseeding.

Prior to cell seeding, sterilized dPMSs were immersed in cell culture media and incubated overnight in cell culture incubator (37 °C; 5% CO_2). Cells were then seeded into custom-built stainless steel O-rings (10 mm inner diameter) placed on top of the dPMS. For lateral cell seeding, 2×10^5 cells in 30 μL of cell culture medium were seeded on one side of the dPMS restrained by the O-ring and incubated in humidified cell culture incubator (37 °C; 5% CO_2) for 4 h before adding another 2 mL of cell culture medium for continuing culture. For bilateral cell seeding, dPMSs were flipped 4 h after one side seeding to receive cells at same density on the other side. The bilaterally seeded dPMSs were cultured in transwell inserts (6 well, 8 μm pore size: Corning, New York, NY, USA) to ensure sufficient supply of cell culture medium to both sides. For both seeding methods, cells were cultured for up to 5 days with media change every 2 days.

2.5. Cell Morphology and Proliferation.

Cell morphology and proliferation were assessed at days 1, 3, and 5 after seeding. For cell morphology assessment, live cells were stained with Calcein AM (2 μM) and cell nuclei were stained with Hoechst 33342 (1:1000). The stained cells were observed using Olympus FluoView FV1000 confocal microscope (Carl Zeiss, Oberkochen, Germany). Cell proliferation was measured using Quant-iT PicoGreen dsDNA assay kit (Molecular Probes, Eugene, OR, USA) according to the manufacturer's recommendations. First, the total DNA content was extracted and purified from the samples using QIAamp DNA mini kit (Qiagen, Valencia, CA, USA). The DNA content solution was then stained with PicoGreen fluorescent nucleic acid dye. The relative fluorescence intensity was quantitatively measured at 480 nm excitation and 520 nm emission using a Synergy H1 hybrid microplate reader (Bio-Tek Instruments, Winooski, VT, USA). Equal number of cells cultured under same conditions were used as controls. All experiments were performed in triplicate.

2.6. Cell Infiltration.

For lateral cell seeding experimental group, cell infiltration distance was assessed in 300 and 600 μm dPMSs on 1, 3, and 5 days of culture. On the day of the experiment, the samples were rinsed with 1× PBS twice and then stained with Calcein AM (2 μM) and Hoechst 33342 (1:1000) for 30 min in humidified cell culture incubator. After incubation, the dPMSs were thoroughly washed with 1× PBS, and fluorescent images were captured using confocal microscope (Carl Zeiss). In brief, Calcein AM and Hoechst 33342 were excited at 488 and 405 nm, respectively, with an argon ion laser and corresponding emissions were recorded at

500−545 nm for Calcein AM and 425−475 nm for Hoechst 33342. The fluorescence signal of cells were then measured from periphery toward the center of dPMS to obtain equidistant Z-stack images (7 μm apart) using Olympus Fluoview software (version 3.1.a). The number of images acquired in each Z-stack image was used to measure the total migration distance of the seeded cells in dPMS. All experiments were performed in triplicate. For bilateral cell seeding experimental group, the total cell distribution in 600 and 900 μm dPMSs after 1 day and 5 days of culture was demonstrated by cell nuclei staining using VECTASHIELD mounting medium with DAPI.

2.7. Histology.

Tissue samples were fixed in 4% (w/v) paraformaldehyde for 2 days at room temperature. Next, samples were dehydrated through graded series of 70%, 95%, and 100% ethanol, followed by two changes of xylenes and three changes of paraffin wax dipping for 1 h each using a tissue processor (Leica ASP300S; Leica, Buffalo Grove, IL, USA). Subsequently, the processed tissues were embedded in paraffin wax in embedding module (Leica EG1150H; Leica, Buffalo Grove, IL, USA) and sectioned into 10 μm thick slices using a microtome (ThermoFisher Scientific, Waltham, MA, USA). For staining, the tissue sections were deparaffinized with xylenes, dehydrated with anhydrous ethanol, and stained using a Hematoxylin and Eosin Kit (H&E; American MasterTech Scientific, Lodi, CA, USA) according to manufacturer's recommendations.

2.8. Immunofluorescence Staining.

Immunofluorescence staining was performed to detect cardiovascular differentiation of cells after being cultured on dPMS. Paraffin-embedded sections (6−8 μm) were deparaffinized using xylenes and rehydrated by histology grade ethanol. Following rehydration, heat mediated antigen retrieval with 1× citrate buffer (pH 6.0; Abcam, Cambridge, MA, USA) was performed at 100 °C for 15 min. The tissue sections were then permeabilized using 0.1% or 0.2% Triton X/PBS solution as needed and blocked with 5% normal goat serum (Abcam, Cambridge, MA, USA) for 45 min. Prior to staining, all primary and secondary antibodies were diluted at a desired concentration using blocking solution containing 5% normal goat serum. For dPMS seeded with rASCs, the tissue sections were incubated at 4 °C for 20−22 h with the following primary antibodies: von Willebrand factor (vWF; 1:50), CD31 (1:50), and VE cadherin (1:50). Similarly, dPMS seeded with hMSCs were incubated with primary antibodies for alpha smooth muscle actin (α-SMA; 1:100), vimentin (1:500), cardiac troponin I (1:400), GATA4 conjugated with Alexa Fluor 647 (1:50), von Willebrand Factor (1:50), CD31 (1:50), and VE cadherin (1:50). After incubation, the tissue sections were extensively rinsed with 1× PBS and incubated with appropriate goat derived secondary antibody conjugated with either Alexa Fluor 488 or 647 (1:100) for 2 h at room temperature. Finally, the tissue sections were stained using VECTASHIELD mounting medium with DAPI for nuclei staining. Fluorescence images were captured with an inverted AxioVision A1 microscope (Carl Zeiss). Following the same protocol, positive controls were prepared with either native tissue or appropriate positive cell lines and negative controls were prepared without primary antibodies.

2.9. Statistical Analyses.

All experimental data were presented as mean ± standard deviation (SD). Statistical analysis was performed with one-way analysis of variance (ANOVA) and Tukey's post hoc test with 95% confidence intervals to determine significant differences among the experimental groups using GraphPad Prism 5 software (GraphPad Software Inc., La Jolla, CA, USA). *p*-Value less than 0.05 was considered to be statistically significant.

3. RESULTS

3.1. Characterization of dPMS.

The dPMS was obtained by tissue slicing following decellularization. Decellularization of the porcine cardiac tissue was performed according to the methods described in the Materials and Methods. After 2.5 weeks of decellularization using the detergent solution, porcine cardiac tissue turned into white color indicating the successful removal of cellular components (Figure 1A). Quantitative DNA analysis showed that the decellularized porcine cardiac tissue had a significant reduction in DNA content compared with the native myocardium (~30 vs ~400 ng DNA/mg wet tissue). ECM proteins, such as collagen and GAG, were assessed and the results were consistent with our previous studies demonstrating the retention of ECM proteins in the decellularized cardiac tissue.[20] dPMS was generated by cryosectioning of decellularized porcine cardiac tissue to desired thickness (300, 600, and 900 μm). The obtained dPMSs preserved the morphological integrity and showed increased transparency compared with native porcine cardiac tissue slice at the same thickness (Figure 1B,C). H&E staining further revealed the complete removal of cells and well preservation of cardiac ECM in the obtained dPMS (Figure 1D,E).

3.2. Cell Attachment and Proliferation on dPMS.

hMSCs and rASCs were used to test cell attachment and proliferation on dPMSs. First, 2×10^5 cells were seeded on one side of dPMS and cultured for up to 5 days. After initial seeding, both cell types were then attached to dPMSs within 6 h and the attached cells were elongated to form spindle shape (Figure 2A). We noticed that a significant amount of cells leaked through the dPMSs after cell seeding and attached to the bottom of cell culture flask. The cell seeding efficiency (percentage of cells attached to dPMS) was found to be dependent on cell type and the thickness of dPMSs. For 300 μm dPMS, the cell seeding efficiencies of hMSCs and rASCs were 33% and 24%, respectively. For 600 μm dPMS, the seeding efficiencies of hMSCs and rASCs were 28% and 27%, respectively. Cells attached to dPMS showed high viability (~88%) according to our results from live/dead cytotoxicity staining. In terms of cell proliferation, the total cell number was quantified at days 1, 3, and 5 by measuring cells within the dPMSs as well as cells grown on the bottom of cell culture flasks. The number of cells, which were either seeded on cell culture flask or attached to the flask after leaking out of dPMSs, are represented in the blue color bars. The number of cells that lived in the dPMSs are presented in the red color bars (for 300 μm dPMS) and green color bars (for 600 μm dPMS), respectively. The error bar on top of each color bar represents the statistic error of each cell group (Figure 2B,C). Cells seeded on 300 μm dPMS proliferated significantly from day 1 to day 3. Both hMSCs and rASCs within dPMSs had a nearly 2-fold increase at day 3. The number of hMSCs in 300 μm dPMS kept increasing

significantly from day 3 to day 5. However, 300 μm dPMS seeded with rASCs were noticed to have dPMS degradation and cells leaking out, which resulted in the significant reduction of the cell number within the dPMS on day 5. Cells seeded on 600 μm dPMS did not show significant growth from day 1 to days 3 and 5, which is similar to the control group where cells were cultured on cell culture plate at the same density.

3.3. Lateral Cell Infiltration in dPMS.

To evaluate the cell infiltration in dPMS, hMSCs and rASCs were seeded on one side of dPMSs for up to 5 days and the cell migration distances were compared between each experiment group (Figure 3A). Cells showed distinct infiltration patterns when seeded on dPMSs with different thickness (Figure 3B). After 5 days of culture, the total migration distance of hMSCs and rASCs seeded on 300 μm dPMSs increased significantly compared with the migration distance on day 1 (~173 vs ~120 μm for hMSCs; ~218 vs 155 μm for rASCs). In contrast, there was no significant difference of the total migration distance from day 1 to day 5 for both hMSCs and rASCs when they were seeded on 600 μm dPMSs. Not only the thickness of dPMSs played a role, we also found that cell types affected cell infiltration. When both cell types were cultured on 300 μm dPMSs for 5 days, the total migration distance of rASCs was significantly longer than that of hMSCs (~218 vs ~173 μm).

3.4. Bilateral Cell Infiltration in dPMS.

hMSCs and rASCs were seeded on both sides of 600 μm dPMSs and cultured in a cell culture insert for up to 5 days to assess bilateral cell infiltration in dPMS (Figure 4A). The bilateral cell seeding efficiencies of hMSCs and rASCs on 600 μm dPMS were 21.07% and 21.43% respectively, which is higher than lateral seeding. One day after bilateral seeding, cells infiltrated from both sides and met in the center of dPMS regardless of cell types (Figure 4B). Because the average thickness of dPMS 1 day after cell seeding is about ~560 μm, the maximum migration distance of cells from either side was at least ~280 μm when they were seeded bilaterally. This is dramatically farther than when cells were seeded from one side of 600 μm dPMS, where cells migrated for up to ~106 μm from the seeding side of dPMS on day 1 and afterward (Figure 3B). After 5 days of bilateral seeding, cells infiltrated through the 600 μm dPMS with significantly increased cell numbers (Figure 4B). The thickness of dPMSs were also noticeably decreased 5 days after bilateral infiltration of cells. The average thickness reduction of dPMS was ~36% for hMSCs and ~50% for rASCs during the 5 day cell infiltration period. The enhanced cell infiltration and proliferation observed above was not shown on cells bilaterally seeded on 900 μm dPMS (Figure 4C). hMSCs showed similar proliferation rate and migration distance in 900 μm dPMS no matter if they were seeded laterally or bilaterally.

3.5. Cardiovascular Differentiation of Infiltrated Cells in dPMS.

Vascular differentiation of hMSCs and rASCs were examined using immunofluorescence staining after the cells were bilaterally seeded onto 600 μm dPMSs for up to 7 days. The expression of endothelial cell markers including CD31, VE cadherin (vascular endothelial cadherin), and von Willebrand factor (vWF) on both cell types were assessed and compared (Figure 5A−C). VE cadherin expressions were observed on both hMSCs and rASCs from

day 1 to day 7. CD31, which is considered to be an early endothelial marker, was clearly expressed on rASCs seeded on dPMS after 3 days. However, it was not detected on hMSCs during the 7 day culture period. Instead, hMSCs had robust vWF expression as early as 1 day after seeding while rASCs did not show any vWF expression until day 5. For both cell types, the positive staining cells were distributed throughout the dPMSs and not limited to the areas near the edges of the slices. hMSCs bilaterally seeded on 600 μm dPMSs also showed high expression of α-SMA (Figure 5D). No cardiac fibroblast and cardiomyocyte differentiation from hMSCs have been detected, which were evidenced by the negative stainings of vimentin, cardiac troponin I, and GATA4 (Figure 5E−G).

4. DISCUSSION

Decellularized cardiac tissue (dCT) has demonstrated great potential in cardiac repair and regeneration. A cellular cardiac patch derived from dCT has improved heart function in both acute and chronic myocardial infarction models.[23] The underlying mechanisms have been suggested to be related to mechanical support provided by the matching mechanical properties of dCT and endogenous progenitor cells recruitment triggered by factors released during dCT mild degradation.[24–26] In addition, as a potent biological scaffold, dCT enables recellularization with selected cell populations.[13,27,28] Human cardiac-progenitor cells (hCPCs), bone-marrow hMSCs, human umbilical vein endothelial cells (HUVECs), and H9c1 and HL-1 cardiomyocytes have been seeded in vitro on dCT derived from human heart. The results prove dCT as a biocompatible scaffold that retains three-dimensional architecture and vascularity. It promotes cardiac gene expression in stem cells and organizes existing cardiomyocytes into nascent muscle showing electrical coupling.[29] However, despite the mounting promising results, effectively recellularized dCT has not been achieved. Limited achievements have been made in terms of using dCT to construct biomimetic cardiac tissue in vitro for disease diagnosis and drug screening as well as using dCT as a highly efficient cell delivery platform for cardiac therapy. One of the major hurdles in dCT recellularization is insufficient vascularization, which leads to poor cell viability after cells are seeded into dCT.[2]

In this study, we strive to develop a simple and effective prevascularization strategy for dCT. We envision in the future that successfully prevascularized dCT could be used as a powerful platform to construct an in vitro 3D cardiac tissue model and fabricate a functional cardiac patch. We focused on finding answers for three specific questions during our strategy development: (1) What is the optimal thickness of the dCT which can maintain the 3D structure of dCT and allow maximal recellularization? (2) What is the best cell source to vascularize dCT? (3) What is the most efficient cell seeding method to allow high efficiency and uniform cell seeding for successful prevascularization. dCT obtained from porcine heart has been chosen for our study due to the abundant resource and xenotransplantation potential. Porcine dCT has been sliced into various thickness (300, 600, and 900 μm) to compare their recellularization capability. Our results suggest that within the chosen thickness range, regardless of thickness, dPMS supports cell attachment and survival. However, cell seeding efficiency and proliferation rate are thickness dependent. Thinner dPMS (300 μm) tends to have more cells leaking out of the scaffold and therefore has lower seeding efficiency compared with thicker dPMSs (600 and 900 μm). However, attached cells

demonstrated higher proliferation rate on 300 μm dPMS, probably because of the sufficient nutrient supply to the cells from diffusion. MSCs and ASCs are the two most popular stem cell types used in inducing vascularization.[30] Both MSCs and ASCs have been proven to be able to differentiate into endothelial and vascular cells in vitro and induce angiogenesis after in vivo transplantation.[13,31,32] When used to recellularize dPMS for vascularization, these two stem cell types show distinct responses. At the same cell amount and culture conditions, dPMSs are degraded clearly faster by ASCs than MSCs and 300 μm dPMS will lose the scaffold physical integrity 5 days after seeding of 2×10^5 ASCs. The thickness of 600 μm dPMS will reduce more than 50% after bilaterally seeding of 4×10^5 ASCs. While under the same condition, MSCs have very mild degradation of dPMSs, both MSCs and ASCs show dPMS induced vascular differentiation by expressing endothelial cell markers. However, compared with ASCs, MSCs do not express early endothelial cell marker (CD31) but have robust expression of mature endothelial cell marker (vWF) since day 1. MSCs when seeded on 600 μm dPMS also highly express α-SMA, which has become an accepted marker of vessel maturity. All these data indicate that hMSCs may undergo accelerated endothelial differentiation and maturation. Therefore, MSCs are a better choice than ASCs to be used to revascularize dPMSs. No cardiac fibroblast or cardiomyocyte differentiation of MSCs have been detected when they are cultured on dPMSs. This matches with published results from other research groups showing the limited potency of MSCs in term of cardiac differentiation when chemical inducers were not employed.[33,34]

One of the most significant findings of this study is that bilateral seeding of MSCs on 600 μm dPMS will increase cell seeding efficiency and infiltration distance. Seeding cells from both sides of the dPMS provides more area for cell attachment, which leads to improved seeding efficiency. When MSCs are seeded from one side of the 600 μm dPMS, they stopped infiltration toward the inner region of the scaffold at day 1 and maintained the migration distance around ~106 μm throughout the 5 day culture period. This may be due to cell sensing of insufficient nutrient and oxygen supply at the center of the scaffold caused by diffusion limitation.[3,7,35–37] Surprisingly, when MSCs are seeded to the 600 μm dPMS from both sides, they traveled farther than 106 μm and reached to the center of the scaffold at day 1. We suspect that the enhanced cell infiltration is triggered by paracrine factors secreted by MSCs. MSCs have been reported to secrete many types of cytokines and growth factors including chemokines such as stromal cell-derived factor 1 (SDF-1) that proves to mobilize MSCs.[38,39] When we bilaterally seed MSCs on 900 μm dPMS, no enhanced cell infiltration has been observed. Cells tend to stay near the edge of the scaffold and refused to migrate toward the center of the scaffold. This observation indirectly supports our suspicion whether cells can receive signaling from cells seeded on the other side affecting their infiltration distance. We plan to investigate the possible paracrine factors secreted by MSCs that may cause the enhanced infiltration in our future studies.

One of the limitations of this study is that all of the above observations are from static seeding. Many published results have demonstrated that dynamic seeding using perfusion bioreactor will significantly increase the uniformity of cell distribution in the scaffold and enhance cell infiltration into a thick construct.[40–43] In future studies, we will incorporate a perfusion bioreactor into our prevasularization strategy development as well as other dynamic seeding options. In addition, mechanical properties of the developed

prevascularized dPMS (preV-dPMS) are very critical for the outcomes of future cardiac application. The capability of preV-dPMS to maintain the overall cardiac ECM mechanical behavior is very important not only in serving as local biomechanical cues for the delivered cells but also in providing the needed reinforcement for the infarcted region of the heart to increase cardiac function. In future studies, we plan to thoroughly investigate the mechanical properties of the developed preV-dPMS and if necessary optimize them to match cardiac ECM mechanical properties before testing their efficacy in animal models.

5. CONCLUSIONS

A simple and practical strategy to fabricate prevascularized biological scaffold for cardiac tissue engineering was explored using decellularized porcine cardiac tissue slice, stem cells, and bilateral cell seeding. Compared with ASCs, MSCs proved to be a better stem cell choice to be used to vascularize dPMS. First, MSCs showed accelerated endothelial differentiation and maturation when cultured in dPMS. Second, unlike ASCs, MSCs did not induce fast dPMS degradation during the 7 day culture period. dPMSs supported cell attachment and survival. Cell seeding efficiency increased and proliferation rate decreased when the thickness of dPMS increased from 300 to 600 μm. Bilateral cell seeding further increased the cell seeding efficiency. When cells were laterally seeded on thicker dPMSs (600 and 900 μm), cell infiltration reached a plateau at day 1 and the infiltration distance was significantly shorter than cells seeded on 300 μm dPMSs. However, when hMSCs were bilaterally seeded onto 600 μm dPMSs, enhanced cell infiltration was clearly observed. These attractive results indicate the potential of using bilateral seeding of hMSCs and 600 μm dPMSs to develop prevascularized dPMSs for cardiac tissue engineering.

ACKNOWLEDGMENTS

We greatly thank the financial support from the National Institutes of Health (1R15HL122949 to G.Z.). We thank Dr. William Landis's group from Polymer Science department at the University of Akron (UA) for allowing us to use their histology facility and the Chemical and Biomolecular Engineering department at UA for letting us use the confocal microscope.

REFERENCES

(1). Laschke MW; Menger MD Prevascularization in Tissue Engineering: Current Concepts and Future Directions. Biotechnol. Adv 2016, 34 (2), 112–121. [PubMed: 26674312]

(2). Novosel EC; Kleinhans C; Kluger PJ Vascularization Is the Key Challenge in Tissue Engineering. Adv. Drug Delivery Rev 2011, 63 (4), 300–311.

(3). Sarig U; Nguyen EB-V; Wang Y; Ting S; Bronshtein T; Sarig H; Dahan N; Gvirtz M; Reuveny S; Oh SKW; Scheper T; Boey YCF; Venkatraman SS; Machluf M Pushing the Envelope in Tissue Engineering: Ex Vivo Production of Thick Vascularized Cardiac Extracellular Matrix Constructs. Tissue Eng., Part A 2015, 21 (9−10), 1507–1519.

(4). Chen X; Aledia AS; Ghajar CM; Griffith CK; Putnam AJ; Hughes CCW; George SC Prevascularization of a Fibrin-Based Tissue Construct Accelerates the Formation of Functional Anastomosis with Host Vasculature. Tissue Eng., Part A 2009, 15 (6), 1363–1371. [PubMed: 18976155]

(5). Muscari C; Giordano E; Bonafe F; Govoni M; Guarnieri C Strategies Affording Prevascularized Cell-Based Constructs for Myocardial Tissue Engineering. Stem Cells Int 2014, 2014 (i), 1–8.

(6). Li D-Q; Li M; Liu P-L; Zhang Y-K; Lu J-X; Li J-M Improved Repair of Bone Defects With Prevascularized Tissue-Engineered Bones Constructed in a Perfusion Bioreactor. Orthopedics 2014, 37 (10), 685–690. [PubMed: 25275969]

(7). Lovett M; Lee K; Edwards A; Kaplan DL Vascularization Strategies for Tissue Engineering. Tissue Eng., Part B 2009, 15 (3), 353–370.

(8). Kaully T; Kaufman-Francis K; Lesman A; Levenberg S Vascularization–the Conduit to Viable Engineered Tissues. Tissue Eng., Part B 2009, 15 (2), 159–169.

(9). Rouwkema J; Rivron NC; van Blitterswijk CA Vascularization in Tissue Engineering. Trends Biotechnol 2008, 26 (8), 434–441. [PubMed: 18585808]

(10). Perets A; Baruch Y; Weisbuch F; Shoshany G; Neufeld G; Cohen S Enhancing the Vascularization of Three-Dimensional Porous Alginate Scaffolds by Incorporating Controlled Release Basic Fibroblast Growth Factor Microspheres. J. Biomed. Mater. Res 2003, 65A (4), 489–497.

(11). Chen RR; Silva EA; Yuen WW; Mooney DJ Spatio-Temporal VEGF and PDGF Delivery Patterns Blood Vessel Formation and Maturation. Pharm. Res 2007, 24 (2), 258–264. [PubMed: 17191092]

(12). Hoshiba T; Lu H; Kawazoe N; Chen G Decellularized Matrices for Tissue Engineering. Expert Opin. Biol. Ther 2010, 10 (12), 1717–1728. [PubMed: 21058932]

(13). Scarritt ME; Pashos NC; Bunnell BA A Review of Cellularization Strategies for Tissue Engineering of Whole Organs. Front. Bioeng. Biotechnol 2015, 3, 43. [PubMed: 25870857]

(14). Fu RH; Wang YC; Liu SP; Shih TR; Lin HL; Chen YM; Sung JH; Lu CH; Wei JR; Wang ZW; Huang SJ; Tsai CH; Shyu WC; Lin SZ Decellularization and Recellularization Technologies in Tissue Engineering. Cell Transplant 2014, 23 (4−5), 621–630. [PubMed: 24816454]

(15). Holt-Casper D; Theisen JM; Moreno AP; Warren M; Silva F; Grainger DW; Bull DA; Patel AN Novel Xeno-Free Human Heart Matrix-Derived Three-Dimensional Scaffolds. J. Transl. Med 2015, 13, 194. [PubMed: 26084398]

(16). Wang Q; Yang H; Bai A; Jiang W; Li X; Wang X; Mao Y; Lu C; Qian R; Guo F; Ding T; Chen H; Chen S; Zhang J; Liu C; Sun N Functional Engineered Human Cardiac Patches Prepared from Nature's Platform Improve Heart Function after Acute Myocardial Infarction. Biomaterials 2016, 105, 52–65. [PubMed: 27509303]

(17). Ott HC; Matthiesen TS; Goh S-K; Black LD; Kren SM; Netoff TI; Taylor D. a. Perfusion-Decellularized Matrix: Using Nature's Platform to Engineer a Bioartificial Heart. Nat. Med 2008, 14 (2), 213–221. [PubMed: 18193059]

(18). Wang B; Tedder ME; Perez CE; Wang G; de Jongh Curry AL; To F; Elder SH; Williams LN; Simionescu DT; Liao J Structural and Biomechanical Characterizations of Porcine Myocardial Extracellular Matrix. J. Mater. Sci.: Mater. Med 2012, 23 (8), 1835–1847. [PubMed: 22584822]

(19). Seif-Naraghi SB; Horn D; Schup-Magoffin PJ; Christman KL Injectable Extracellular Matrix Derived Hydrogel Provides a Platform for Enhanced Retention and Delivery of a Heparin-Binding Growth Factor. Acta Biomater 2012, 8 (10), 3695–3703. [PubMed: 22750737]

(20). Jeffords ME; Wu J; Shah M; Hong Y; Zhang G Tailoring Material Properties of Cardiac Matrix Hydrogels To Induce Endothelial Differentiation of Human Mesenchymal Stem Cells. ACS Appl. Mater. Interfaces 2015, 7 (20), 11053–11061. [PubMed: 25946697]

(21). Shah M; George RL; Evancho-Chapman MM; Zhang G Current Challenges in Dedifferentiated Fat Cells Research. Organogenesis 2016, 12, 119–127. [PubMed: 27322672]

(22). Gimble JM; Katz AJ; Bunnell BA Adipose-Derived Stem Cells for Regenerative Medicine. Circ. Res 2007, 100 (9), 1249–1260. [PubMed: 17495232]

(23). Sarig U; Sarig H; De-Berardinis E; Chaw S; Nguyen EBV; Ramanujam VS; Thang VD; Al-Haddawi M; Liao S; Seliktar D; Kofidis T; Boey FYC; Venkatraman SS; Machluf M Natural Myocardial ECM Patch Drives Cardiac Progenitor Based Restoration Even after Scarring. Acta Biomater 2016, 44, 209–220. [PubMed: 27545814]

(24). Teodori L; Costa A; Marzio R; Perniconi B; Coletti D; Adamo S; Gupta B; Tarnok A Native Extracellular Matrix: A New Scaffolding Platform for Repair of Damaged Muscle. Front. Physiol 2014, 5, 218. [PubMed: 24982637]

(25). He M; Callanan A Comparison of Methods for Whole-Organ Decellularization in Tissue Engineering of Bioartificial Organs. Tissue Eng., Part B 2013, 19 (3), 194–208.

(26). Beattie AJ; Gilbert TW; Guyot JP; Yates AJ; Badylak SF Chemoattraction of Progenitor Cells by Remodeling Extracellular Matrix Scaffolds. Tissue Eng., Part A 2009, 15 (5), 1119–1125. [PubMed: 18837648]

(27). Badylak SF; Taylor D; Uygun K Whole-Organ Tissue Engineering: Decellularization and Recellularization of Three-Dimensional Matrix Scaffolds. Annu. Rev. Biomed. Eng 2011, 13 (1), 27–53. [PubMed: 21417722]

(28). Cutts J; Nikkhah M; Brafman DA Biomaterial Approaches for Stem Cell-Based Myocardial Tissue Engineering. Biomarker Insights 2015, 10, 77–90. [PubMed: 26052226]

(29). Sánchez PL; Fernández-Santos ME; Costanza S; Climent AM; Moscoso I; Gonzalez-Nicolas MA; Sanz-Ruiz R; Rodríguez H; Kren SM; Garrido G; Escalante JL; Bermejo J; Elizaga J; Menarguez J; Yotti R; Peŕez del Villar C; Espinosa MA; Guillem MS; Willerson JT; Bernad A; Matesanz R; Taylor DA; Fernández-Avilés F Acellular Human Heart Matrix: A Critical Step toward Whole Heart Grafts. Biomaterials 2015, 61, 279–289. [PubMed: 26005766]

(30). Pill K; Hofmann S; Redl H; Holnthoner W Vascularization Mediated by Mesenchymal Stem Cells from Bone Marrow and Adipose Tissue: A Comparison. Cell Regener 2015, 4, 8.

(31). Kadota Y; Yagi H; Inomata K; Matsubara K; Hibi T; Abe Y; Kitago M; Shinoda M; Obara H; Itano O; Kitagawa Y Mesenchymal Stem Cells Support Hepatocyte Function in Engineered Liver Grafts. Organogenesis 2014, 10 (2), 268–277. [PubMed: 24488046]

(32). Fischer LJ; McIlhenny S; Tulenko T; Golesorkhi N; Zhang P; Larson R; Lombardi J; Shapiro I; DiMuzio PJ Endothelial Differentiation of Adipose-Derived Stem Cells: Effects of Endothelial Cell Growth Supplement and Shear Force. J. Surg. Res 2009, 152 (1), 157–166. [PubMed: 19883577]

(33). Silva GV Mesenchymal Stem Cells Differentiate into an Endothelial Phenotype, Enhance Vascular Density, and Improve Heart Function in a Canine Chronic Ischemia Model. Circulation 2005, 111 (2), 150–156. [PubMed: 15642764]

(34). Galli D; Vitale M; Vaccarezza M Bone Marrow-Derived Mesenchymal Cell Differentiation toward Myogenic Lineages: Facts and Perspectives. BioMed Res. Int 2014, 2014, 1–6.

(35). Griffith CK; Miller C; Sainson RCA; Calvert JW; Jeon NL; Hughes CCW; George SC Diffusion Limits of an in Vitro Thick Prevascularized Tissue. Tissue Eng 2005, 11 (1−2), 257–266. [PubMed: 15738680]

(36). Griffith CK; George SC The Effect of Hypoxia on in Vitro Prevascularization of a Thick Soft Tissue. Tissue Eng., Part A 2009, 15 (9), 2423–2434. [PubMed: 19292659]

(37). Radisic M; Malda J; Epping E; Geng W; Langer R; Vunjak-Novakovic G Oxygen Gradients Correlate with Cell Density and Cell Viability in Engineered Cardiac Tissue. Biotechnol. Bioeng 2006, 93 (2), 332–343. [PubMed: 16270298]

(38). Landry Y; Lê O; Mace KA; Restivo TE; Beauséjour CM Secretion of SDF-1α by Bone Marrow-Derived Stromal Cells Enhances Skin Wound Healing of C57BL/6 Mice Exposed to Ionizing Radiation. J. Cell. Mol. Med 2010, 14 (6b), 1594–1604. [PubMed: 19725920]

(39). Tang J; Wang J; Yang J; Kong X; Zheng F; Guo L; Zhang L; Huang Y Mesenchymal Stem Cells over-Expressing SDF-1 Promote Angiogenesis and Improve Heart Function in Experimental Myocardial Infarction in Rats☆. Eur. J. Cardio-Thoracic Surg 2009, 36 (4), 644–650.

(40). Crabbé A; Liu Y; Sarker SF; Bonenfant NR; Barrila J; Borg ZD; Lee JJ; Weiss DJ; Nickerson CA Recellularization of Decellularized Lung Scaffolds Is Enhanced by Dynamic Suspension Culture. PLoS One 2015, 10 (5), e0126846. [PubMed: 25962111]

(41). Villalona GA; Udelsman B; Duncan DR; McGillicuddy E; Sawh-Martinez RF; Hibino N; Painter C; Mirensky T; Erickson B; Shinoka T; Breuer CK Cell-Seeding Techniques in Vascular Tissue Engineering. Tissue Eng., Part B 2010, 16 (3), 341–350.

(42). Haykal S; Salna M; Zhou Y; Marcus P; Fatehi M; Frost G; Machuca T; Hofer SOP; Waddell TK Double-Chamber Rotating Bioreactor for Dynamic Perfusion Cell Seeding of Large-Segment Tracheal Allografts: Comparison to Conventional Static Methods. Tissue Eng., Part C 2014, 20 (8), 681–692.

(43). Alvarez-Barreto JF; Linehan SM; Shambaugh RL; Sikavitsas VI Flow Perfusion Improves Seeding of Tissue Engineering Scaffolds with Different Architectures. Ann. Biomed. Eng 2007, 35 (3), 429–442. [PubMed: 17216348]

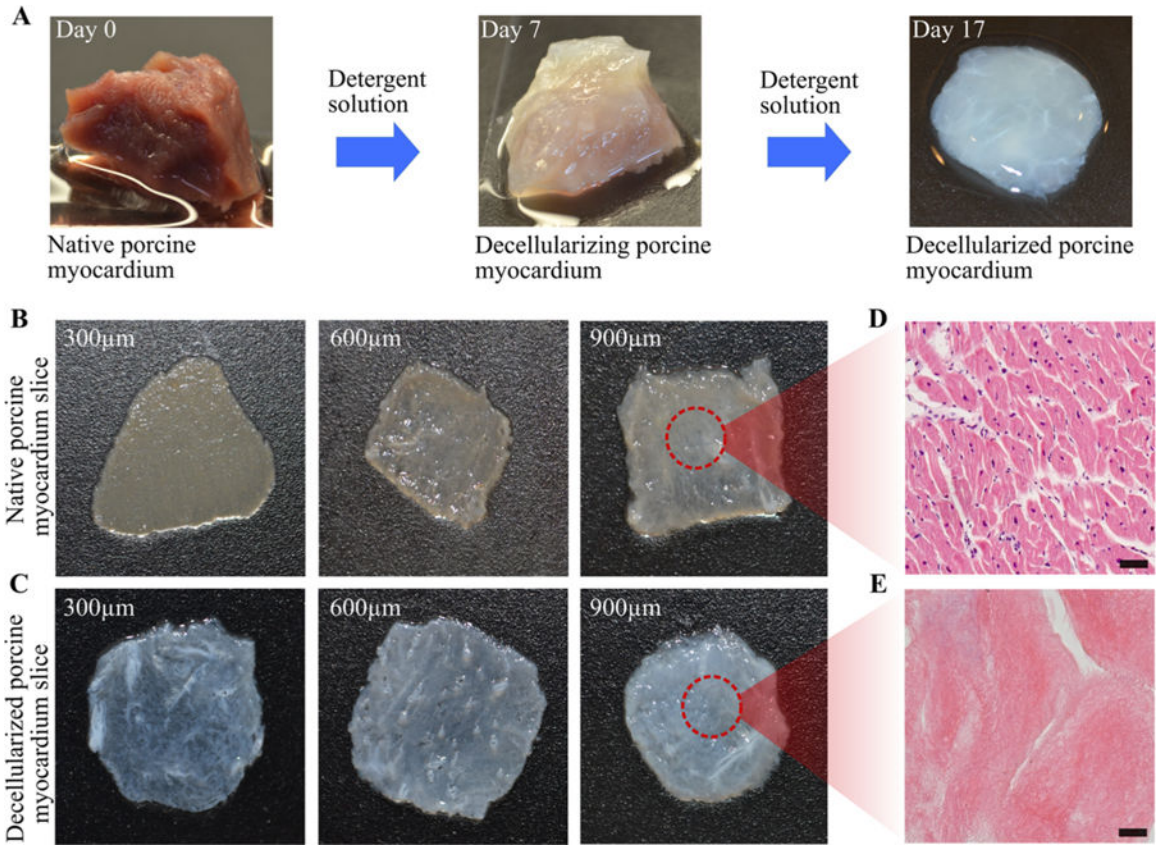

Figure 1.

Native and decellularized porcine myocardium slices. (A) Representative images of porcine myocardium tissue during decellularization process at days 0, 7, and 17. (B) Native porcine myocardium slices at 300, 600, and 900 μm thicknesses. (C) Decellularized porcine myocardium slices at 300, 600, and 900 μm thicknesses. (D) H&E staining of native porcine myocardium slice and (E) H&E staining of decellularized porcine myocardium slice (E). Scale bar 50 μm.

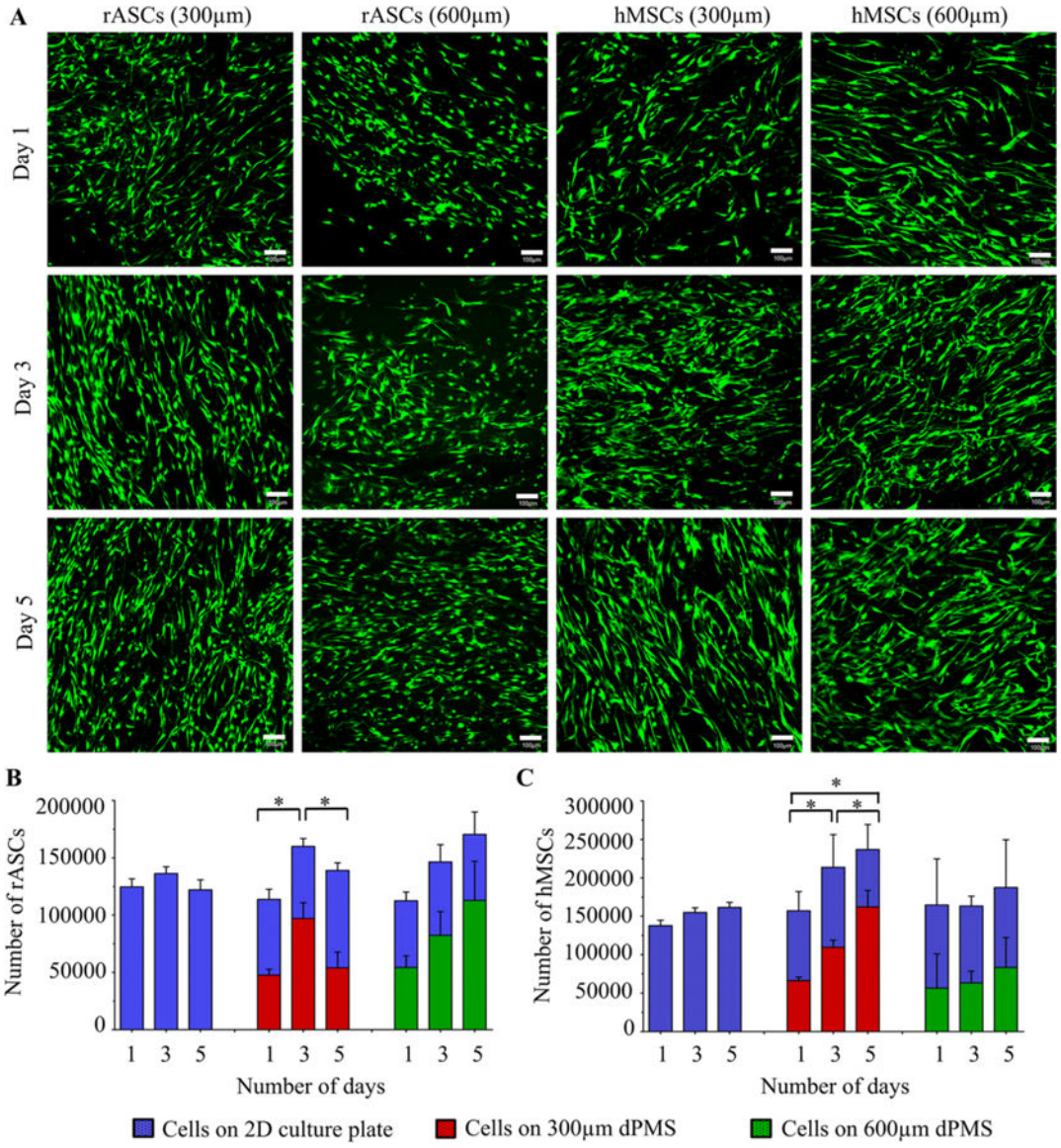

Figure 2.

Cell attachment and proliferation on 300 and 600 μm dPMSs. (A) Representative z-stacked confocal images showing morphology of seeded hMSCs and rASCs on 300 and 600 μm dPMSs at days 1, 3, and 5. Cells were stained with Calcein AM. Scale bar 100 μm. (B,C) Cell proliferation quantification of seeded hMSCs and rASCs. Data were expressed as means ± SD (n = 3 for each sample). * represents the statistical significant difference with p value <0.05.

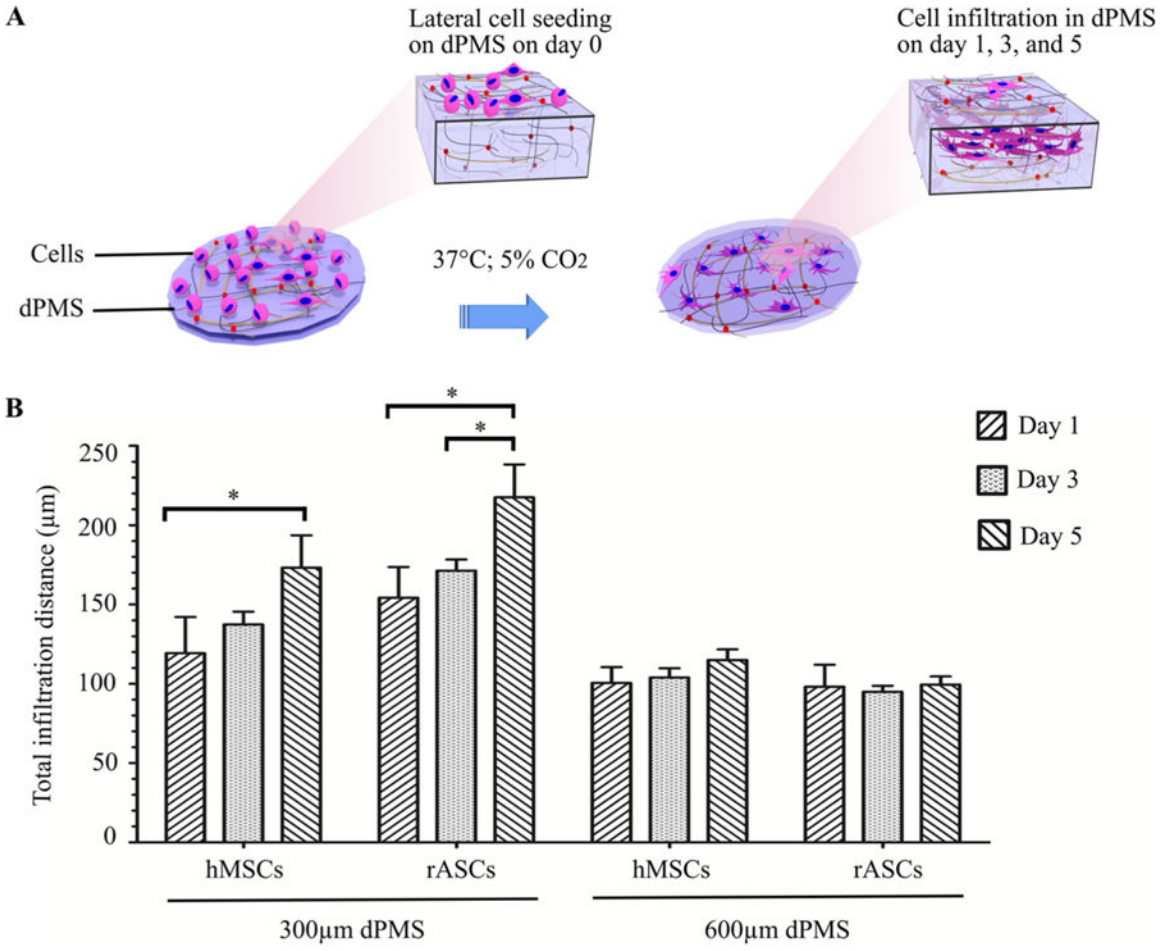

Figure 3.

hMSCs and rASCs infiltration in 300 and 600 μm dPMSs. (A) Schematic diagram of the experiment procedure showing lateral cell infiltration in dPMS. (B) Migration distance comparison between hMSCs and rASCs seeded on 300 and 600 μm dPMSs after 1, 3, and 5 days culture. * represents the statistically significant difference between experiment groups with p value <0.05.

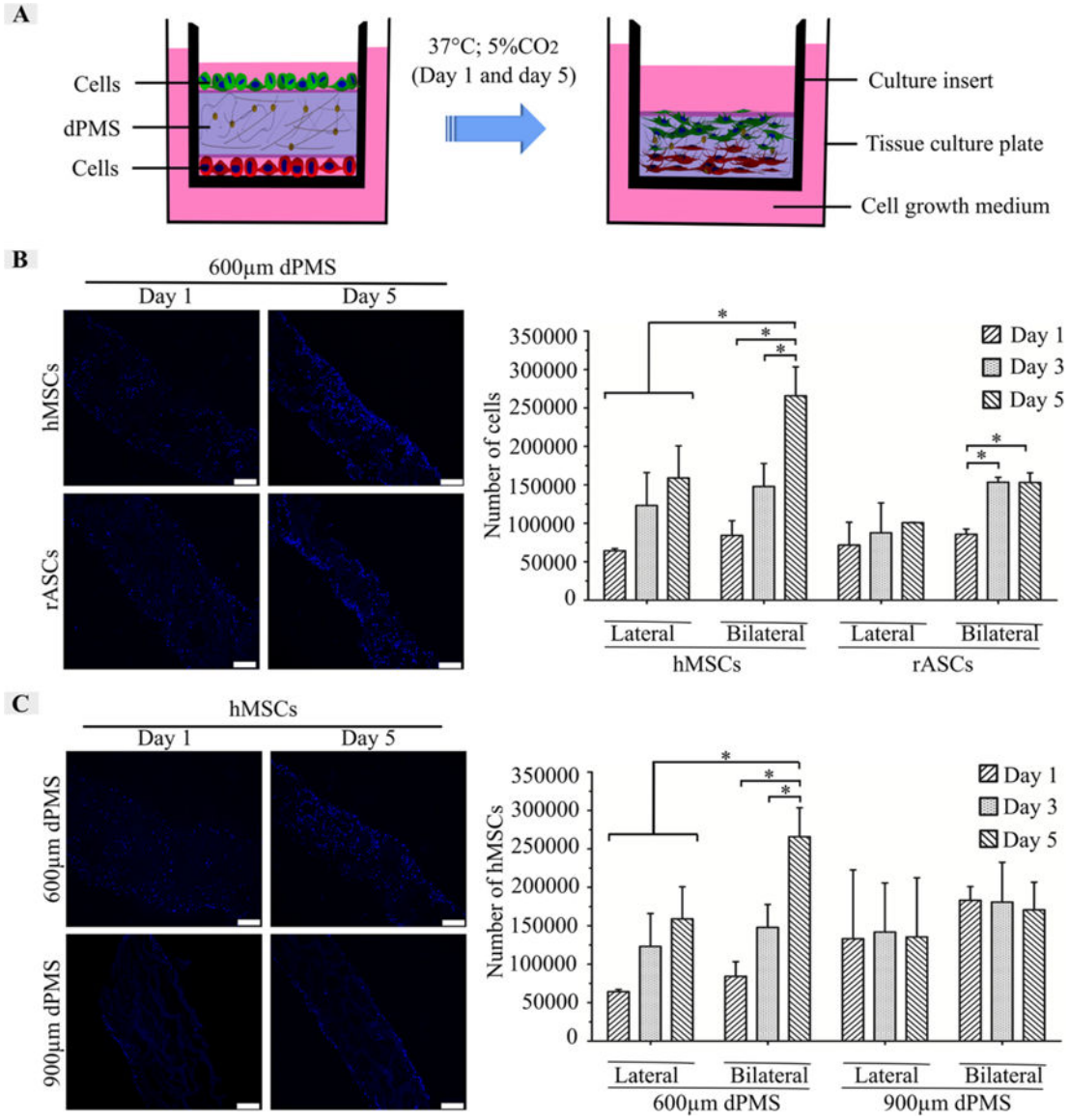

Figure 4.

Cell infiltration and proliferation in bilaterally seeded 600 and 900 μm dPMSs. (A) Schematic diagram to show bilateral cell seeding and culture conditions. (B) DAPI staining to demonstrate the infiltration of bilaterally seeded hMSCs and rASCs in 600 μm dPMS. Cell proliferation comparison of laterally and bilaterally seeded hMSCs and rASCs in 600 μm dPMS at days 1, 3, and 5. (C) DAPI staining of bilaterally seeded hMSCs showing cell infiltration in 900 μm dPMS. Cell proliferation of laterally and bilaterally seeded hMSCs in 900 μm dPMS at days 1, 3, and 5. * represents the statistically significant difference with p value <0.05. Scale bar 200 μm.

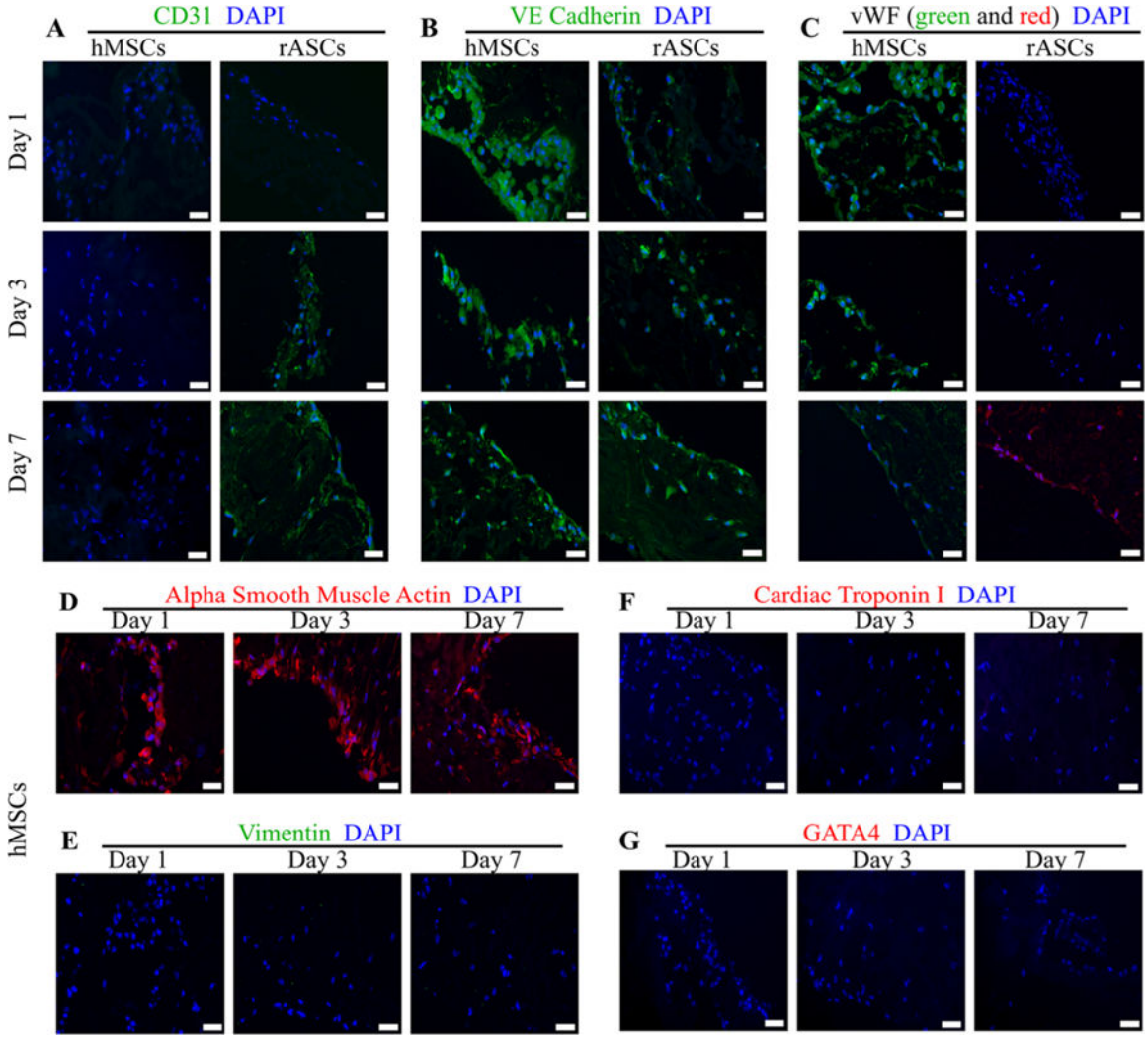

Figure 5.

Cardiovascular differentiation assessment of bilaterally seeded hMSCs and rASCs in 600 μm dPMS. (A−C) Immunofluorescence staining of hMSCs and rASCs for early endothelial marker CD31, VE cadherin, and late endothelial marker vWF. (D−G) Immunofluorescence staining of hMSCs for α-SMA, vimentin, cardiac troponin I, and GATA 4. Scale bar 50 μm.